

RAPID DETECTION OF TETRODOTOXIN USING SURFACE-ENHANCED RAMAN SPECTROSCOPY AND $Fe_3O_4/SiO_2/Au$ GOLD/MAGNETIC NANOPARTICLES****Jing Neng, Xujun Wang, Kan Jia, Peilong Sun ***

Ocean College, Zhejiang University of Technology, Department of Food Science and Technology, Hangzhou, Zhejiang 310014, China; e-mail: sun_pl@zjut.edu.cn

Fe_3O_4 nanoparticles were first modified with tetraethoxysilane to form Fe_3O_4/SiO_2 nanoparticles, followed by the addition of 3-aminopropyltriethoxysilane and 3-thiolpropyltriethoxysilane to introduce $-NH_2$ and $-SH$ groups to the surface of Fe_3O_4/SiO_2 nanoparticles. Gold nanoparticles were further assembled on the surface of Fe_3O_4/SiO_2 via the electrostatic adsorption of $-NH_2$ and the Au-S bond to produce stable core-shell $Fe_3O_4/SiO_2/Au$ gold/magnetic nanoparticles. These $Fe_3O_4/SiO_2/Au$ gold/magnetic nanoparticles were characterized by a variety of techniques such as transmission electron microscopy (TEM) and energy dispersive X-ray spectroscopy (EDX), and afterwards conjugated with tetrodotoxin antibodies (Ab) and used as a Raman active substrate ($Fe_3O_4/SiO_2/Au-Ab$) with Rhodamine B (RhB)-labeled tetrodotoxin antibody as a Raman reporter (Ab-RhB). Upon mixing these reagents with tetrodotoxin (TTX), a sandwich complex [$Fe_3O_4/SiO_2/Au-Ab \cdots TTX \cdots Ab-RhB$] was generated due to the specific antibody-antigen interactions. The immunocomplex was subsequently separated by an externally applied magnetic source and concentrated into a pellet point, where the laser interrogation of the pellet produced a strong signal characteristic of RhB. The logarithmic intensity of the signal was found to be proportional to the concentration of TTX with a limit of detection of 0.01 $\mu g/mL$ and a detection linearity range of $\sim 0.01-0.5 \mu g/mL$. The established method eliminates the complicated procedures of traditional centrifuging, column separation, and incubation and achieves a rapid detection of tetrodotoxin with improved detection sensitivity.

Keywords: surface-enhanced Raman spectroscopy, rapid detection, tetrodotoxin, magnetic nanoparticles.

БЫСТРОЕ ОБНАРУЖЕНИЕ ТЕТРОДОТОКСИНА С ИСПОЛЬЗОВАНИЕМ СПЕКТРОСКОПИИ ГИГАНТСКОГО КОМБИНАЦИОННОГО РАССЕЯНИЯ И $Fe_3O_4/SiO_2/Au$ ЗОЛОТЫХ/МАГНИТНЫХ НАНОЧАСТИЦ**J. Neng, X. Wang, K. Jia, P. Sun ***

УДК 535.375;620.3

Океанический колледж, Технологический университет Чжэцзян, Ханчжоу, Чжэцзян, 310014, Китай; e-mail: sun_pl@zjut.edu.cn

(Поступила 28 декабря 2016)

Наночастицы Fe_3O_4 модифицированы тетраэтоксисилоном с образованием наночастиц (НЧ) Fe_3O_4/SiO_2 , после чего к ним добавлены 3-аминопропил- и 3-тиолпропил-триэтоксисилан, чтобы внедрить NH_2 - и SH -группы на поверхность наночастиц Fe_3O_4/SiO_2 . Затем на их поверхности дополнительно размещались НЧ Au посредством электростатической адсорбции NH_2 и Au-S. В результате получены состоящие из ядра и оболочки стабильные магнитные НЧ $Fe_3O_4/SiO_2/Au$, которые исследованы методами просвечивающей электронной микроскопии (ТЕМ) и энергодисперсионного рентгеновского анализа. Синтезированные НЧ соединены с тетродотоксин-антителами (Ab) и использованы как КР-активный субстрат ($Fe_3O_4/SiO_2/Au-Ab$), где в качестве КР-метки выступают меченные родамином В (RhB) тетродотоксин-антитела (Ab-RhB). При соединении этих реагентов с тетродотоксином (TTX) генерируется сэндвич-комплекс [$Fe_3O_4/SiO_2/Au-Ab \cdots TTX \cdots Ab-RhB$], обусловленный специфическими взаимодействиями антиген-антитело. Полученный иммунокомплекс отделили

** Full text is published in JAS V. 85, No. 1 (<http://springer.com/10812>) and in electronic version of ZhPS V. 85, No. 1 (http://www.elibrary.ru/title_about.asp?id=7318; sales@elibrary.ru).

внешним магнитным полем и концентрировали в точечную гранулу, которая при лазерном воздействии давала сильный сигнал, характерный для RhB. Обнаружено, что логарифм интенсивности сигнала пропорционален концентрации TTX с пределом обнаружения 0.01 мкг/мл и диапазоном линейности детектирования ~0.01–0.5 мкг/мл. Разработанный метод обладает повышенной чувствительностью обнаружения и не требует сложных процедур традиционного центрифугирования, колонного разделения и инкубации, что обеспечивает быстрое обнаружение тетродотоксина.

Ключевые слова: спектроскопия гигантского комбинационного рассеяния, быстрое обнаружение, тетродотоксин, магнитные наночастицы.

Introduction. Tetrodotoxin (TTX) is an alkaloid that exists in puffer fish and other animals, such as xanthid crabs and flatworms [1]. With a molecular formula of $C_{11}H_{17}N_3O_8$ (molecular weight: 319.27), TTX is recognized as one of the most toxic neurotoxins and nonprotein toxoids found in nature [2]. It is highly chemically and thermally stable and can only be hydrolyzed and broken down at elevated temperatures in alkaline conditions.

Current approaches used to detect TTX include biological methods involving mice, thin layer chromatography (TLC), electrophoresis, and high-performance liquid chromatography (HPLC) [3]. Although the mouse bioassay is a legally approved method for the quantitative determination of TTX in Japan, it is labor-intensive and suffers from poor repeatability and lack of specificity. TLC and electrophoresis are useful for the detection of TTX, but not for its quantitative determination because of their insufficient sensitivity and reproducibility. HPLC has been used to qualitatively and quantitatively detect TTX [4, 5]; however, the sample pretreatment is time-consuming and requires complicated laboratory work, which makes it unsuitable for rapid on-site detection.

Surface-enhanced Raman spectroscopy (SERS) has been widely used in surface, biological, and analytical sciences over the past few decades. In 1974, Fleischmann and co-workers [6] first detected the enhanced Raman signal of pyridine on the surface of a rough silver electrode. Van Duyne et al. [7] later revealed that the Raman signal of pyridine molecules attached to the surface of rough silver electrodes was about 10^6 times stronger than that of the same amount of the compound in solution. Owing to their high surface enhanced Raman scattering effects, gold and silver nanoparticles (NPs) are generally used in SERS as Raman-active substrates [8]. Under ideal conditions, SERS can detect a single molecule of the analyte [9]. Recently, SERS has been developed as a platform for pathogen and biothreat detection, cancer diagnostics [10], DNA and RNA detection [11–13], protein immunoassays [14–18], and food-safety analysis [19–23].

In this work, Fe_3O_4 NPs were first treated with tetraethoxysilane (TEOS) to form Fe_3O_4/SiO_2 NPs; this was then followed by addition of 3-aminopropyltriethoxysilane and 3-thiolpropyltriethoxysilane to introduce $-NH_2$ and $-SH$ onto the surface of the Fe_3O_4/SiO_2 NPs, respectively. Next, Au NPs were assembled on the surface of the Fe_3O_4/SiO_2 NPs through electrostatic interactions between the $-NH_2$ and the Au-S bond to produce stable core-shell $Fe_3O_4/SiO_2/Au$ gold/magnetic NPs. These $Fe_3O_4/SiO_2/Au$ gold/magnetic NPs were conjugated with TTX antibody (Ab) and used as a Raman-active substrate ($Fe_3O_4/SiO_2/Au-Ab$) with Rhodamine B (RhB)-labeled TTX antibody as a Raman reporter (Ab-RhB). A sandwich complex [$Fe_3O_4/SiO_2/Au-Ab \cdots TTX \cdots Ab-RhB$] was formed on mixing these reagents with TTX, and this complex was subsequently separated with an external magnet and concentrated into a pellet point. TTX was rapidly detected with improved sensitivity over conventional techniques by laser excitation of the pellet. The synthesis and characterization of the $Fe_3O_4/SiO_2/Au$ gold/magnetic NPs, the effect of the reaction conditions on the SERS effect, and the detection limit for TTX as well as the corresponding linearity range, were investigated.

Experimental. Instruments and reagents. SERS spectra were acquired using a DeltaNu Advantage 785 Raman spectrometer equipped with a microscope and a stage-sample holder. The Raman spectrometer has a laser power of 120 mW at wavelength at 785 nm and a spectral range of 200–2000 cm^{-1} . The prepared $Fe_3O_4/SiO_2/Au$ gold/magnetic NPs were observed on a transmission electron microscope (TEM, Tecnai G2 F30 S-Twin) equipped with an energy dispersive X-ray (EDX) analyzer (JEOL 4000FX), operating at a high acceleration voltage of 300 keV. Ultrasonic oscillator (KQ3200B) was purchased from Kunshan ultrasonic instrument limited company. High-speed desktop centrifuge (TGL-16G) was purchased from Shanghai Anting Scientific Instrument Limited Company.

RhB isothiocyanate (mixed isomers, $C_{29}H_{30}N_3O_3S$) and Fe_3O_4 nanopowder (97%, 50–100 nm) were purchased from Sigma-Aldrich. Gold chloride acid hydrate ($HAuCl_4 \cdot 4H_2O$, 99%) was purchased from Shanghai Siyu Chemical Technology Limited Company. Tetraethoxysilane (TEOS, 99%), sodium citrate ($C_6H_5Na_3O_7 \cdot 2H_2O$, 99%), (3-aminopropyl)triethoxysilane (APTES, 99%), and γ -mercaptopropyl-

triethoxysilane (MPTES, 98%) were obtained from Aladdin. The active ester polyethylene glycol ($\geq 95\%$, NHS-PEG-NHS, $MW = 800$) was purchased from Shanghai Tuoyang Biological Technology Limited Company. Tetrodotoxin (TTX, 1.0 mg) was purchased from Shanghai Yuanye Biotechnology Limited Company. Tetrodotoxin antibody (TTX Ab, 1mg/mL) was purchased from Shanghai Boyan Biological Technology Limited Company. Saxitoxin (STX, 1.0 mg) was purchased from Beijing Pushihua Technology Development Limited Company. All other chemicals were of analytical grade and used without further purification.

Synthesis of $Fe_3O_4/SiO_2/Au$ gold/magnetic nanoparticles. The Fe_3O_4 NP was first modified with silane according to a literature method [24]. Briefly, 4.00 mg of Fe_3O_4 NPs was dispersed in 2 mL of distilled water followed by addition of 10 mL of ethanol and 0.2 mL of anhydrous ammonia. After the solution was ultrasonicated for 5 min, 8 μ L of TEOS was slowly added and the mixture was treated with ultrasonic oscillation for 6 h. The NPs were separated by a magnet and washed with anhydrous ethanol and distilled water, then redispersed in a mixture of 2 mL water, 10 mL ethanol, and 0.2 mL of ammonia. Then 4 μ L of APTES and 4 μ L of MPTES were added to the mixture, which was subjected to ultrasonication for 16 h. The final Fe_3O_4 NPs modified with $-NH_2$ and $-SH$ groups were separated by a magnet, washed with anhydrous ethanol and distilled water, and redispersed in 10 mL of distilled water.

The synthesis of Au NPs is based on a literature method [25]. Briefly, 50 mL of distilled water was heated to $100^\circ C$ under stirring and 100 μ L of sodium citrate solution (w/w 5%) was added into the water. Then 1 mL of distilled water containing 10.00 mg of gold chloride acid hydrate was added dropwise and the solution kept boiling for 3 min. After the solution cooled down to room temperature, Au NPs were collected by centrifuge at 10000 g for 10 min and redispersed in 50 mL of distilled water.

Modified Fe_3O_4 NP solution (4 mL) was mixed with 4 mL of Au NP solution, and the mixture was gently stirred (150 rpm) at room temperature for 6 h. Then the solution was separated by a magnet and washed twice with distilled water to obtain $Fe_3O_4/SiO_2/Au$ NPs.

Synthesis of the TTX Ab conjugated nanoparticles ($Fe_3O_4/SiO_2/Au-Ab$). The above prepared $Fe_3O_4/SiO_2/Au$ gold/magnetic NPs were redispersed in a mixture of 0.5 mL of distilled water, 3.5 mL of ethanol, and 50 μ L of ammonia under ultrasonication. Afterwards, 3 μ L of TEOS and 2 μ L of APTES were slowly added and the solution was treated with ultrasonication for 16 h. Then the $Fe_3O_4/SiO_2/Au$ gold/magnetic NPs were separated with a magnet, washed twice with distilled water, and redispersed in 4 mL of distilled water. NHS-PEG-NHS (1 mg) was dissolved in 1 mL of phosphate buffer (PBS, pH 7.4) and then mixed with 1 mL of above gold magnetic NP solution. The mixture was stirred at room temperature for 6 h to immobilize the PEG-NHS group on the surface of the $Fe_3O_4/SiO_2/Au$ gold/magnetic NPs. After the reaction completed, the modified $Fe_3O_4/SiO_2/Au$ gold/magnetic NPs were collected by a magnet, washed with PBS buffer, and redispersed in 2 mL of PBS containing 0.1 mL of tetrodotoxin antibody solution (1.0 mg/mL). The solution was stirred at room temperature for 6 h, and TTX Ab conjugated NPs $Fe_3O_4/SiO_2/Au-Ab$ were obtained. The NPs were finally separated by a magnet, redispersed in 2 mL of PBS, and stored in the refrigerator at $4^\circ C$.

Synthesis of the RhB-labeled TTX Ab reporter ($Ab-RhB$). RhB isothiocyanate (50 μ g) was dissolved in 0.2 mL of $NaHCO_3$ buffer solution (pH 8.3) and mixed with 0.1 mL of tetrodotoxin antibody (1.0 mg/mL). The mixture was stirred at room temperature for 6 h and then dialyzed against $NaHCO_3$ buffer solution to remove the excess of RhB.

Detection of TTX by the combination of $Fe_3O_4/SiO_2/Au-Ab$ and $Ab-RhB$. The detection assay of TTX was assembled by addition of 50 μ L of $Fe_3O_4/SiO_2/Au-Ab$ solution, 10 μ L of $Ab-RhB$ solution, and 60 μ L of a series of PBS solutions containing dilutions of TTX. The final concentrations of TTX in these solutions are 0.5, 0.1, 0.05, 0.02, 0.01, and 0.005 μ g/mL respectively. Triplicate reactions for each concentration of TTX detection were incubated for 2 h at room temperature and then separated by the application of an external magnet, after which the concentrated pellet material was transferred to a concave slide for laser excitation. RhB spectra were acquired with the baseline off and analyzed using Grams/AITM software. The third strong peak at 1510 cm^{-1} of RhB was used for the quantitative detection of TTX as the strongest peak at 1360 cm^{-1} and the second strong peak at 1275 cm^{-1} were prone to interference with the glass background of slide [26]. The total analysis time was less than 1 h.

Results and discussion. TEM analysis of $Fe_3O_4/SiO_2/Au$ gold/magnetic nanoparticles. Figure 1 shows the TEM images of $Fe_3O_4/SiO_2/Au$ gold/magnetic NPs at different resolutions. Obviously, the large Fe_3O_4 NPs with diameter ranging from 100–200 nm are covered by a layer of small Au NPs. The Au NPs have a diameter of 20–40 nm with narrow size distribution and are closely attached to the surface of Fe_3O_4 NP due to the electrostatic adsorption of $-NH_2$ and the Au-S bond.

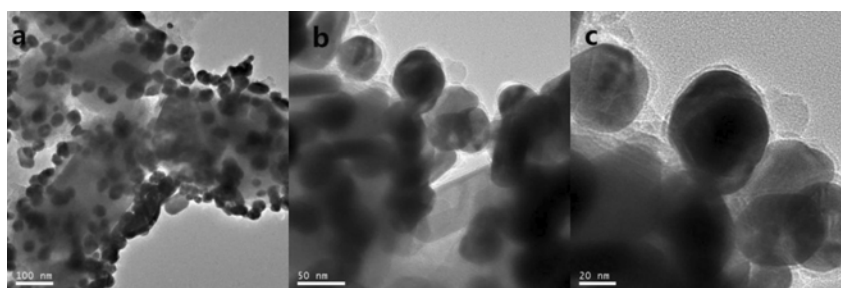


Fig. 1. TEM images of $\text{Fe}_3\text{O}_4/\text{SiO}_2/\text{Au}$ gold/magnetic NPs at different resolutions.

The effects of preparation method of the $\text{Fe}_3\text{O}_4/\text{SiO}_2/\text{Au}$ gold/magnetic nanoparticles on the SERS effect. The effects of three different assembly methods of Au NPs (stirring, shaking, and ultrasonication) coating on Fe_3O_4 magnetic NPs on the SERS effect were investigated and the results are shown in Fig. 2. Figure 2a shows that the $\text{Fe}_3\text{O}_4/\text{Au}$ NPs were assembled by gently stirring the mixture of Au NP solution and Fe_3O_4 NP solution. The Fe_3O_4 magnetic NPs were densely and uniformly covered by a layer of gold NPs. Correspondingly, the Raman scattering intensity of RhB adsorbed on $\text{Fe}_3\text{O}_4/\text{Au}$ NPs was higher than 8000 at the peak of 1510 cm^{-1} (Fig. 2b). The Fe_3O_4 NPs were less densely covered by Au NPs (Fig. 2c) when using shaking instead of the above stirring method, and the corresponding Raman scattering intensity of RhB decreased to about 6500 at 1510 cm^{-1} (Fig. 2d). Only a small amount of gold NPs was attached to the surface of Fe_3O_4 NPs when the mixture of Au and Fe_3O_4 NP solution was treated with ultrasonication (Fig. 2e), and accordingly the Raman scattering intensity was further decreased to lower than 3500 at 1510 cm^{-1} (Fig. 2f), indicating that ultrasonication may cause the gold NPs shedding from the surface of Fe_3O_4 NPs.

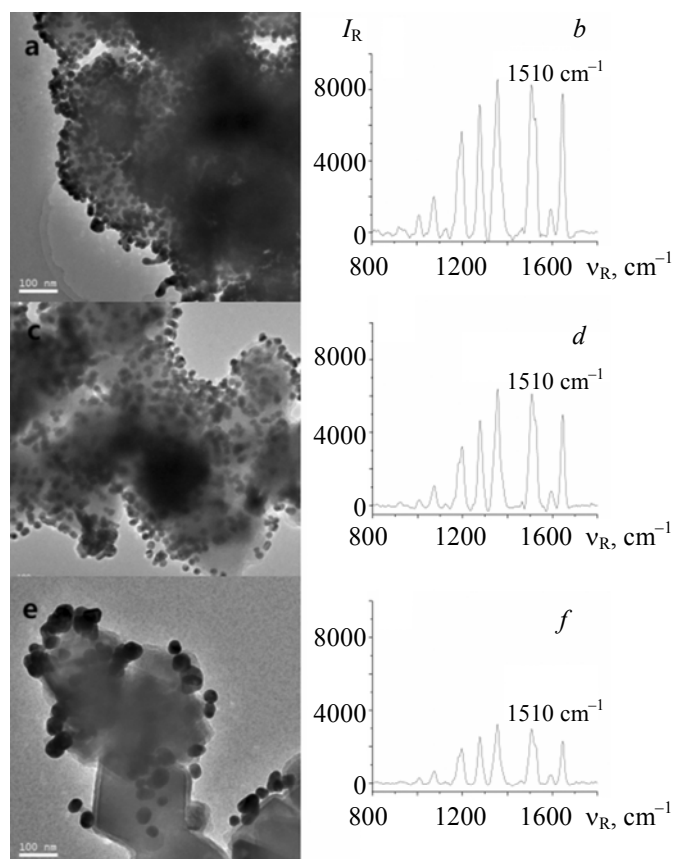


Fig. 2. TEM images (a, c, e) of $\text{Fe}_3\text{O}_4/\text{SiO}_2/\text{Au}$ gold/magnetic NPs prepared by different assembly methods and the corresponding SERS spectra of RhB (b, d, f).

Detection of TTX using $[\text{Fe}_3\text{O}_4/\text{SiO}_2/\text{Au-Ab}\cdots\text{TTX}\cdots\text{Ab-RhB}]$ immunocomplex as a matrix. Figure 3 shows the SERS spectra acquired from the sample. a) containing 50 μL of $\text{Fe}_3\text{O}_4/\text{SiO}_2/\text{Au-Ab}$, 10 μL of Ab-RhB, and 60 μL of 0.1 $\mu\text{g}/\text{mL}$ TTX; b) containing 50 μL of $\text{Fe}_3\text{O}_4/\text{SiO}_2/\text{Au-Ab}$ and 10 μL of Ab-RhB as a blank; and c) containing 50 μL of $\text{Fe}_3\text{O}_4/\text{SiO}_2/\text{Au-Ab}$, 10 μL of Ab-RhB, and 60 μL of 0.1 $\mu\text{g}/\text{mL}$ saxitoxin as a control antigen. Clearly, the spectrum for the sample containing 0.1 $\mu\text{g}/\text{mL}$ TTX (a) demonstrated strong peaks characteristic for RhB at 1275, 1360, 1510, and 1648 cm^{-1} , suggesting that the TTX had been captured due to the formation of $[\text{Fe}_3\text{O}_4/\text{SiO}_2/\text{Au-Ab}\cdots\text{TTX}\cdots\text{Ab-RhB}]$ immunocomplex. The negative control without the addition of TTX (b) produced a background spectrum with only a broad peak centered at 1360 cm^{-1} resulting from the interference of glass slide [26]. This is because there was no antigen-antibody specific interaction that connected $\text{Fe}_3\text{O}_4/\text{SiO}_2/\text{Au-Ab}$ and Ab-RhB together due to the absence of tetrodotoxin. RhB dyes could not be collected, separated, and concentrated to a pellet point by an external magnet and were thus left in the supernatant, resulting in the absence of characteristic peaks of RhB. Saxitoxin has a molecular structure similar to tetrodotoxin, however, the control assay containing 0.1 $\mu\text{g}/\text{mL}$ saxitoxin (c) provided a background spectrum like spectrum b, indicating that the current detection of TTX based on $[\text{Fe}_3\text{O}_4/\text{SiO}_2/\text{Au-Ab}\cdots\text{TTX}\cdots\text{Ab-RhB}]$ immunocomplex has excellent specificity.

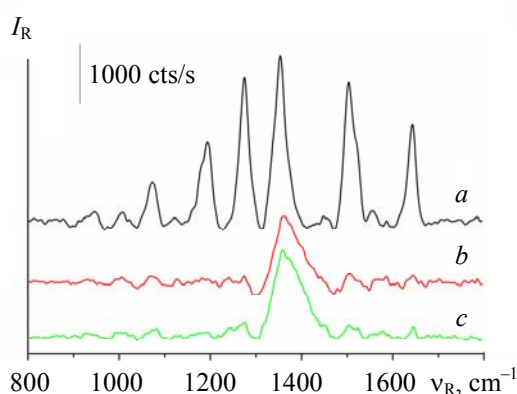


Fig. 3. SERS spectra acquired from the sample. a) Containing 50 μL of $\text{Fe}_3\text{O}_4/\text{SiO}_2/\text{Au-Ab}$, 10 μL of Ab-RhB, and 60 μL of 0.1 $\mu\text{g}/\text{mL}$ TTX; b) containing 50 μL of $\text{Fe}_3\text{O}_4/\text{SiO}_2/\text{Au-Ab}$ and 10 μL of Ab-RhB; c) containing 50 μL of $\text{Fe}_3\text{O}_4/\text{SiO}_2/\text{Au-Ab}$, 10 μL of Ab-RhB, and 60 μL of 0.1 $\mu\text{g}/\text{mL}$ saxitoxin.

Detection sensitivity of TTX using $[\text{Fe}_3\text{O}_4/\text{SiO}_2/\text{Au-Ab}\cdots\text{TTX}\cdots\text{Ab-RhB}]$ immunocomplex as a matrix. The SERS spectra of RhB acquired from the $[\text{Fe}_3\text{O}_4/\text{SiO}_2/\text{Au-Ab}\cdots\text{TTX}\cdots\text{Ab-RhB}]$ immunocomplex with different TTX concentration ranging from 0.005 to 0.500 $\mu\text{g}/\text{mL}$ are shown in Fig. 4. A progressive decrease in the intensity of RhB signature peak was observed when decreasing the TTX concentration from 0.500 to 0.005 $\mu\text{g}/\text{mL}$. As the spectrum obtained from 0.005 $\mu\text{g}/\text{mL}$ of TTX is indistinguishable from background spectra (Fig. 3,b,c), a conservative limit of detection for TTX is set at 0.01 $\mu\text{g}/\text{mL}$.

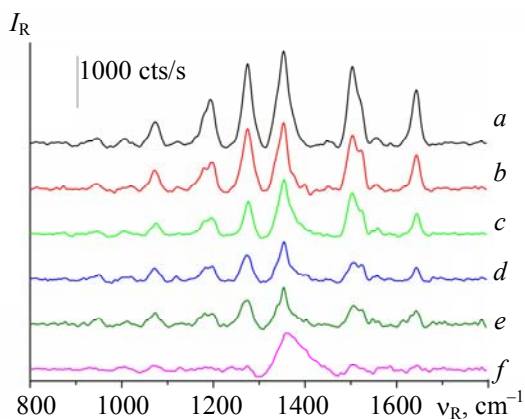


Fig. 4. SERS spectra acquired from the $[\text{Fe}_3\text{O}_4/\text{SiO}_2/\text{Au-Ab}\cdots\text{TTX}\cdots\text{Ab-RhB}]$ immunocomplex with TTX concentration at 0.5 (a), 0.1 (b), 0.05 (c), 0.02 (d), 0.01 (e), and 0.005 $\mu\text{g}/\text{mL}$ (f).

To determine the quantitative response of SERS signaling intensification to TTX detection, a plot of natural logarithm of TTX concentration versus natural logarithm of peak intensity at 1510 cm^{-1} shows that TTX detection is linear within the concentration between 0.01 and 0.5 $\mu\text{g/mL}$. The linear equation is $\ln I_{1510} = 9.347 \ln C_{\text{TTX}} + 0.892$ ($\ln I_{1510}$ is the natural logarithm of peak intensity at 1510 cm^{-1} , $\ln C_{\text{TTX}}$ is the natural logarithm of TTX concentration), and the linear regression yields an R^2 value of 0.9959 for TTX detection.

In order to test and verify the reliability of the standard curve, aqueous samples containing TTX at concentration of 0.50, 0.05, and 0.01 $\mu\text{g/mL}$, were prepared. Each sample was tested three times under the same condition. The analysis of the precision and recovery is shown in Table 1. The test results of TTX recovery is ~ 84.54 – 90.67% , and the relative standard deviation (RSD) is between 2.6 to 11.1%.

TABLE 1. Accuracy and Precision Analysis for the TTX Detection Using $[\text{Fe}_3\text{O}_4/\text{SiO}_2/\text{Au}-\text{Ab}\cdots\text{TTX}\cdots\text{Ab}-\text{RhB}]$ as a Matrix

Concentration under test, $\mu\text{g/mL}$	Measured concentration, $\mu\text{g/mL}$	Average recovery rate, %	RSD, %
0.5	0.448	88.53	5.3
	0.463		
	0.417		
0.05	0.0455	90.67	11.1
	0.0541		
	0.0443		
0.01	0.0119	84.54	2.6
	0.0115		
	0.0121		

Conclusion. This paper demonstrates a rapid detection of TTX by using $\text{Fe}_3\text{O}_4/\text{SiO}_2/\text{Au}$ gold /magnetic NPs conjugated with TTX antibodies as a Raman active substrate ($\text{Fe}_3\text{O}_4/\text{SiO}_2/\text{Au}-\text{Ab}$) and TTX antibody labeled Rhodamine B as Raman reporter ($\text{Ab}-\text{RhB}$). Using an external magnet, the $[\text{Fe}_3\text{O}_4/\text{SiO}_2/\text{Au}-\text{Ab}\cdots\text{TTX}\cdots\text{Ab}-\text{RhB}]$ immunocomplex was separated and concentrated into a pellet point. The laser interrogation of the pellet produced a strong signal of Rhodamine B, and the logarithmic intensity of the signal was found to be proportional to the concentration of TTX within the linear range of ~ 0.01 – 0.5 $\mu\text{g/mL}$. The recovery rate of samples was in the range of ~ 84.54 – 90.67% , and the relative standard deviation was ~ 2.6 – 11.1% .

Acknowledgment. The authors wish to acknowledge the financial support of the National Natural Science Foundation of China (Grant No. 31301483), Zhejiang Provincial Natural Science Foundation of China (Grant No. LY17C200016), Scientific Research Fund of Zhejiang Provincial Education Department (Grant No. Y201329221), and Scientific Research Foundation for the Returned Overseas Chinese Scholars, State Education Ministry.

Conflict of Interest. The authors declare that they have no conflicts of interest in this work. We declare that we do not have any commercial or associative interest that represents a conflict of interest in connection with the manuscript submitted.

REFERENCES

1. E. P. Ragelis, *J. Assoc. Chem.*, **65**, 327–331 (1982).
2. A. S. May, *Chem. Ind.*, **24**, 982–984 (1982).
3. T. Yasumoto, M. Nakamura, Y. Oshima, J. Takahata, *Bull. Jpn. Soc. Sci. Fish.*, **48**, 1481–1483 (1982).
4. J. Huang, M. J. Yan, *Chem. Biotechnol. Lett.*, **17**, 998–1000 (2006).
5. T. Nakayama, S. Tetrakawa, *Anal. Biochem.*, **126**, 153–155 (1982).
6. T. Yasumato, T. Michishita, *Agric. Biol. Chem.*, **49**, 3077–3088 (1985).
7. M. Fleischmann, P. J. Hendra, A. J. Mcquillan, *Chem. Phys. Lett.*, **26**, 163–166 (1974).
8. D. L. Jeanmaire, R. P. V. Duyne, *J. Electroanal. Chem.*, **84**, 1–20 (1977).
9. M. G. Albrecht, J. A. Creighton, *J. Am. Chem.*, **99**, 5215–5217 (2002).
10. N. P. Pieczonka, R. F. Acora, *Chem. Soc. Rev.*, **37**, 946–954 (2008).

11. X. Y. Zhang, J. Zhao, A. V. Whitney, J. W. Elan, R. P. Duyne, *J. Am. Chem. Soc.*, **128**, 10304–10309 (2006).
12. M. Culha, D. Stokes, L. R. Allain, T. Vo-Dinh, *Anal. Chem.*, **75**, 6196–6201 (2003).
13. Y. C. Cao, R. Jia, C. A. Mirkin, *Science*, **297**, 1536–1540 (2002).
14. T. Park, S. Lee, G. H. Seong, J. Choo, E. K. Lee, Y. S. Kim, W. H. Ji, S. Y. Hwang, D. G. Gweon, *Lab Chip*, **5**, 437–442 (2005).
15. M. Y. Sha, S. G. Penn, R. G. Freeman, W. E. Doering, *J. Nanobiotech.*, **3**, 23–30 (2007).
16. Y. C. Cao, R. Jia, J. M. Nam, C. S. Thaxton, C. A. Mirkin, *J. Am. Chem. Soc.*, **125**, 14676–14677 (2003).
17. J. D. Driskell, J. M. Uhlenkamp, R. J. Lipert, M. D. Porter, *Anal. Chem.*, **79**, 4141–4148 (2007).
18. J. L. Gong, Y. Liang, Y. Huang, J. W. Chen, J. H. Jiang, G. L. Shen, R. Q. Yu, *Biosens. Bioelectron.*, **22**, 1501–1507 (2007).
19. J. Neng, M. H. Harpster, H. Zhang, J. O. Mecham, W. C. Wilson, P. Johnson, *Biosens. Bioelectron.*, **26**, 1009 (2010).
20. J. Neng, M. H. Harpster, W. C. Wilson, P. Johnson, *Biosens. Bioelectron.*, **41**, 316 (2013).
21. A. P. Craig, A. S. Franca, J. Irudayaraj, *Annu. Rev. Food. Sci. Technol.*, **4**, 369–380 (2013).
22. J. Zheng, L. He, *Comp. Rev. Food. Sci. Food Safety*, **13**, 317–329 (2014).
23. Y. L. Wang, S. Ravindranath, J. Irudayaraj, *Anal. Bioanal. Chem.*, **399**, 1271–1278 (2011).
24. G. H. Mirzabe, A. R. Keshtkar, *J. Ind. Eng. Chem.*, **26**, 277–285 (2015).
25. G. Frens, *Nature*, **241**, 20–22 (1972).
26. P. Boolchand, M. Jin, D. I. Novita, S. Chakravarty, *J. Raman Spectrosc.*, **38**, 660–672 (2007).